

Compact Dual-Band Wilkinson Power Divider Terminated with Frequency-Dependent Complex Impedances

Xiao Jia, Shaojun Fang, Hongmei Liu*, and Zhongbao Wang

Abstract—In the letter, a compact dual-band Wilkinson power divider (WPD) terminated with frequency-dependent complex impedance (FDCI) is proposed, for the first time. It is composed of two sections of coupled lines, two shunt transmission lines, and a lumped resistor. By using the coupled lines, the FDCI at two bands can be matched. The design equations for the proposed power divider are derived by using the even-odd mode decomposition technology. For verification, a prototype operating at 1.0 GHz and 1.8 GHz was designed, fabricated and measured with different terminal complex impedances at the two bands. The measured results show that the proposed WPD features equal power distribution, good impedance matching/isolation at two frequency bands.

1. INTRODUCTION

Wilkinson power divider (WPD) has been widely used in radio frequency and microwave circuits, such as the feeding network for an array antenna. In recent years, with the development of the multiband wireless communication system, dual-band WPDs have been implemented by using different techniques [1–4]. However, those proposed dual-band WPDs can be only terminated with real impedances. They cannot be used directly for many microwave components such as transistors, diodes, and antennas, where the input or output port is a frequency-dependent complex impedance (FDCI). An extra impedance transformer must be inserted between WPDs and microwave components to achieve impedance matching.

To solve the problem mentioned above, some studies have been focused on the WPDs terminated with complex impedances [5, 6]. In [5], a WPD with equal complex impedances at all ports was presented, and the input port can be matched to $50\ \Omega$ by adding an open stub. In [6], a general design method for WPD was presented. The termination impedances of the output ports are selected as equal complex impedances. The input port can be selected as any value which is independent of the output ports. However, the above WPDs can only work at a single band.

In the letter, a compact dual-band Wilkinson power divider terminated with frequency-dependent complex impedances is presented. The WPD can be matched to $50\ \Omega$ at the input port and equal FDCI at two output ports. Closed-form design equations are derived, and the design procedures are summarized. At last, a dual-band WPD operating at 1 GHz and 1.8 GHz is designed, fabricated, and measured for validation.

2. THEORETICAL ANALYSIS

Figure 1 shows the schematic diagram of the proposed WPD. It is composed of two coupled lines, two shunt transmission lines (TLs), and a lumped resistor. The corresponding characteristic impedances

Received 19 March 2020, Accepted 30 April 2020, Scheduled 24 May 2020

* Corresponding author: Hongmei Liu (lhm323@dlmu.edu.cn).

The authors are with the School of Information Science and Technology, Dalian Maritime University, Dalian, Liaoning 116026, China.

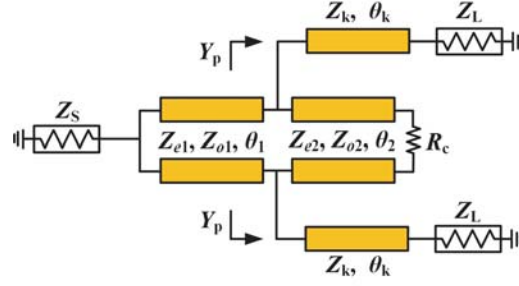


Figure 1. Schematic diagram of the proposed WPD.

and electrical lengths are defined in Fig. 1. The source impedance (Z_S) is a real impedance, and the load impedance (Z_L) is an FDCI. At the two bands f_a and f_b (assuming $f_b \geq f_a$), the load impedances are equal to $R_a + jX_a$ and $R_b + jX_b$, respectively.

According to Fig. 1, Z_L is firstly transformed to Y_p by the stub. Thus, the admittance Y_p at two frequencies can be calculated:

$$Y_p|_{f_a} = \frac{1}{Z_k} \frac{Z_k + j(R_a + jX_a) \tan(\theta_k)}{R_a + jX_a + jZ_k \tan(\theta_k)} \quad (1a)$$

$$Y_p|_{f_b} = \frac{1}{Z_k} \frac{Z_k + j(R_b + jX_b) \tan(u\theta_k)}{R_b + jX_b + jZ_k \tan(u\theta_k)} \quad (1b)$$

where $u = f_b/f_a$ ($m \geq 0$) is the band ratio.

Since the circuit in Fig. 1 is symmetric in structure, even-odd mode decomposition technology is applied to obtain the equivalent half circuits, as shown in Fig. 2. The WPD should be matched at each port and isolated between two output ports. Thus, the even-mode [Fig. 2(a)] and odd-mode [Fig. 2(b)] half circuits are matched by satisfying the following equations:

$$2Z_S = Z_{e1} \frac{\frac{1}{Z_{e1}} - \left(B_p + \frac{\tan \theta_2}{Z_{e2}} \right) \tan \theta_1 + jG_p \tan \theta_1}{G_p + j \left(B_p + \frac{\tan \theta_1}{Z_{e1}} + \frac{\tan \theta_2}{Z_{e2}} \right)} \quad (3a)$$

$$\frac{R_c}{2} = Z_{o2} \frac{\frac{1}{Z_{o2}} - \left(B_p - \frac{\cot \theta_1}{Z_{o1}} \right) \tan \theta_2 + jG_p \tan \theta_2}{G_p + j \left(B_p - \frac{\cot \theta_1}{Z_{o1}} + \frac{\tan \theta_2}{Z_{o2}} \right)} \quad (3b)$$

where G_p and B_p are the real and imaginary parts of the admittance Y_p , respectively.

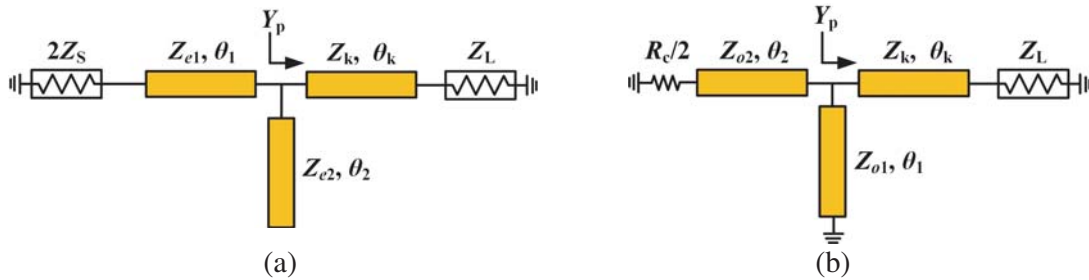


Figure 2. Equivalent sub-circuits of the WPD. (a) Even-mode. (b) Odd-mode.

Further, the design equations can be established as

$$(1 - 2Z_S G_p)Z_{e2} = (Z_{e2}B_p + \tan \theta_2)Z_{e1} \tan \theta_1 \quad (4a)$$

$$G_p Z_{e1} \tan \theta_1 = 2 \left(B_p + \frac{\tan \theta_1}{Z_{e1}} + \frac{\tan \theta_2}{Z_{e2}} \right) Z_S \quad (4b)$$

$$(2 - G_p R_c)Z_{o1} = 2(Z_{o1}B_p - \cot \theta_1)Z_{o2} \tan \theta_2 \quad (4c)$$

$$G_p Z_{o2} \tan \theta_2 = \left(B_p - \frac{\cot \theta_1}{Z_{o1}} + \frac{\tan \theta_2}{Z_{o2}} \right) \frac{R_c}{2} \quad (4d)$$

To design a dual-band WPD, 8 equations have to be solved according to Eq. (3), which increase the complexity of the calculation greatly. For simplification, the constraint of the electrical length of the coupled line is added [7], as illustrated in Eqs. (5a) and (5b). Further, to ensure dual-band operation, the limit of B_p is also added, as shown in Eq. (5c). Using Eq. (5c), it is found that the value of Y_p at f_a is conjugated with that at f_b , yielding $Y_p|_{f_a} = Y_p^*|_{f_b}$

$$\tan(\theta_{1,f_a}) = -\tan(\theta_{1,f_b}) \quad (5a)$$

$$\tan(\theta_{2,f_a}) = -\tan(\theta_{2,f_b}) \quad (5b)$$

$$B_{p,f_a} = -B_{p,f_b} \quad (5c)$$

To solve Eqs. (5a) and (5b), the following expressions are obtained.

$$\theta_1 = \frac{n\pi}{1 + f_b/f_a} \quad (n = 1, 2, \dots) \quad (6a)$$

$$\theta_2 = \frac{m\pi}{1 + f_b/f_a} \quad (m = 1, 2, \dots) \quad (6b)$$

where n and m are any integer greater than zero.

According to the relationship of $Y_p|_{f_a} = Y_p^*|_{f_b}$, the characteristic impedance Z_k and electrical length θ_k of the TL can be presented by applying Eq. (1).

$$Z_k = \sqrt{R_a R_b + X_a X_b + \frac{X_a + X_b}{R_b - R_a} (R_a X_b - R_b X_a)} \quad (7a)$$

$$\theta_k = \frac{c\pi + \arctan \frac{Z_k(R_a - R_b)}{R_a X_b - R_b X_a}}{1 + f_b/f_a} \quad (7b)$$

where c is the arbitrary integer, but a small value should be selected to achieve a compact structure.

Applying Eq. (3), the even- and odd-mode characteristics impedances of the coupled lines in Fig. 1 can be obtained as

$$Z_{e1} = \sqrt{\frac{2a^2 Z_S + 2Z_S - 4G_p Z_S^2}{a^2 G_p}} \quad (8a)$$

$$Z_{e2} = \frac{ab Z_{e1}}{1 - 2Z_S G_p - a Z_{e1} B_p} \quad (8b)$$

$$Z_{o1} = \frac{2b Z_{o2}}{2ab B_p Z_{o2} + a R_c G_p - 2a} \quad (8c)$$

$$Z_{o2} = \sqrt{\frac{2b^2 R_c - G_p R_c^2 + 2R_c}{4b^2 G_p}} \quad (8d)$$

where

$$a = \tan \frac{n\pi}{1 + u} \quad (9a)$$

$$b = \tan \frac{m\pi}{1 + u} \quad (9b)$$

Equations (5)–(7) describe the design parameters of the dual-band WPD, which is terminated with FDCI. In Eqs. (4)–(6), the values of parameters m , n , and the isolation resistor (R_c) can be selected arbitrarily. The physical implementation is the only restriction. For easy fabrication of the coupled line, weak coupling is preferred, which can be performed by selecting suitable values of m , n , and R_c . For example, a suitable value of Z_{e1} can be selected by adjusting the parameter m , while by changing n , the value of Z_{e2} can be adjusted. Finally, the suitable values of Z_{o1} and Z_{o2} are determined by varying R_c . Due to the flexibility of determining the even- and odd mode impedance of the coupled line, strong coupling for some certain frequency ratio and complex terminations can be avoided.

In the following, the design procedures of the proposed WPD are provided

1) The terminal impedances Z_S and Z_L at two frequencies are firstly determined, selecting the low frequency as design frequency.

2) According to Eq. (6), the values of Z_k and θ_k are calculated.

3) From Eqs. (6a) and (6b), the values of θ_1 and θ_2 are selected, where suitable n and m are determined to ensure that the coupled lines are physically achievable.

4) The values of the even-mode and odd-mode characteristic impedances are calculated by Eq. (7).

Using the above procedures, several examples with different complex terminal impedances and frequency ratios are designed. The calculated circuit parameters are listed in Table 1.

Table 1. The calculated circuit parameters of the WPD with different terminal impedance and frequency ratio.

Terminal impedance	Z_k (Ω)	θ_k ($^\circ$)	Z_{e1} (Ω)	Z_{o1} (Ω)	θ_1 ($^\circ$)	Z_{e2} (Ω)	Z_{o2} (Ω)	θ_2 ($^\circ$)	R_c (Ω)
62.6 + j10.1 Ω at 0.8 GHz; 88.2 + j12.3 Ω at 1.2 GHz	74.4	106.5	64.7	47.6	216	89.1	46.1	144	25
72.4 + j16.4 Ω at 1 GHz; 58.4 – j25.3 Ω at 1.8 GHz	45.2	59.7	61.2	42.2	64.3	63.5	49.4	128.6	100
88.2 + j12.3 Ω at 1.2 GHz; 44.4 + j24.0 Ω at 2.4 GHz	53.9	78.8	41.6	32.2	60	55.3	29.7	120	40
62.6 + j10.1 Ω at 0.8 GHz; 45.1 – j12.4.0 Ω at 2.0 GHz	50.4	144.1	67.6	55.3	102.9	51.9	45.5	205.7	100

3. DESIGN PROCEDURE AND EXPERIMENTAL RESULTS

In this section, an example is designed to verify the aforementioned design theory and method. The band ratio is taken as $f_b/f_a = 1.8$. The load impedances are 72.4 + j16.4 Ω at 1 GHz and 58.4 – j25.3 Ω at 1.8 GHz (the second example in Table 1). The source impedance is 50 Ω . According to the calculated circuit parameters in Table 1, a simulation is carried out, and the simulated frequency responses of the designed WPD are shown in Fig. 3. Dual-band characteristic is clearly observed around 1 GHz and 1.8 GHz as desired. The expected performances can be observed at two bands simultaneously, such as an equal power split, the perfecting impedance matching at all ports, and the perfect isolation between two output ports. Further, a discussion on the frequency ratio limitation is carried out based on the designed example. Fig. 4 shows the even- and odd-mode characteristic impedances as a function of the frequency ratio f_b/f_a . It is observed that the values of Z_{e1} , Z_{o1} , and Z_{o2} change slightly with the frequency ratio, while the varying of Z_{e2} is quick. Considering the fabrication limits, Z_{e2} should be less than 130 Ω and more than the value of Z_{o2} . Thus, the frequency ratio for the designed example is in the range of 1.5 ~ 2.1.

The designed WPD is implemented using microstrip technology on a Rogers 4350B substrate having dielectric $\epsilon_r = 3.66$, dissipation factor $\tan \delta = 0.003$, and substrate height = 0.762 mm. Fig. 5 shows the layout and photograph of the designed prototypes. The optimized dimensions are $w_0 = 1.66$ mm, $l_0 = 15$ mm, $w_1 = 1.59$ mm, $s_1 = 0.56$ mm, $l_1 = 30.03$ mm, $w_2 = 1.47$ mm, $s_2 = 0.74$ mm, $l_2 = 60.23$ mm, $w_3 = 1.94$ mm, $l_3 = 28.43$ mm, $R_c = 100$ Ω .

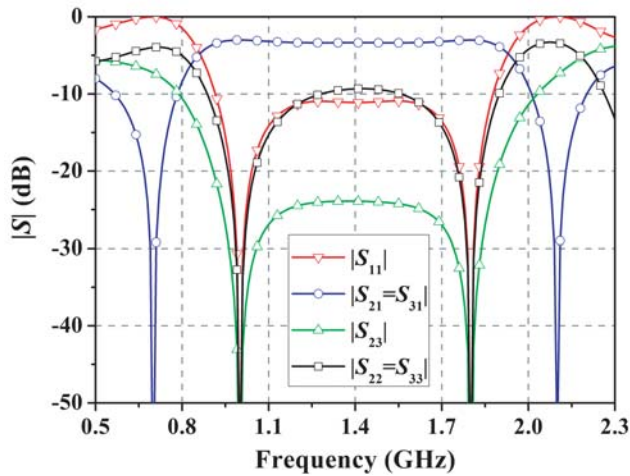


Figure 3. Simulated frequency responses of the WPD with $f_b/f_a = 1.8$.

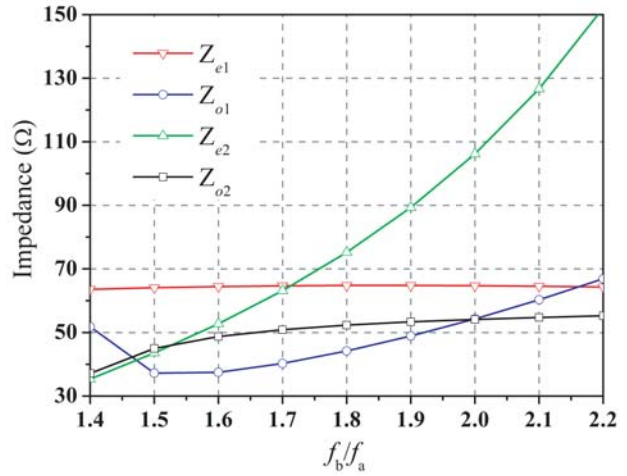


Figure 4. Computed even- and odd-mode characteristic impedances versus frequency ratio.

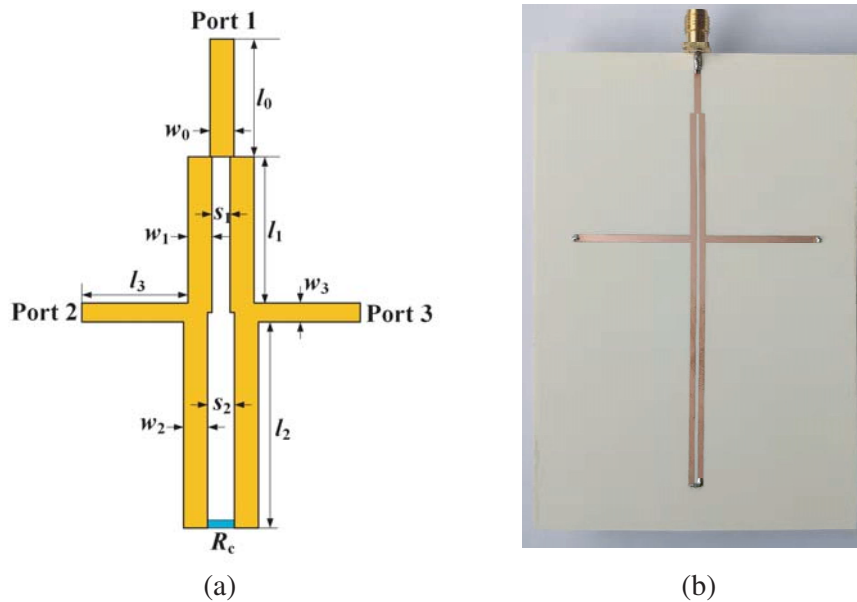


Figure 5. The proposed WPD. (a) Layout. (b) Photograph.

Since ports 2 and 3 of WPD are terminated with complex impedances, the S -parameters are difficult to measure with a $50\text{-}\Omega$ measurement system. In the design, the results of the fabricated WPD are obtained by impedance conversion. Firstly, ports 2 and 3 of the WPD are welded with a $50\text{-}\Omega$ SMA connector, and S -parameters are measured using the $50\text{-}\Omega$ measurement system (vector network analyzer). It is noticed that the measured results are the results for $50\text{-}\Omega$ terminated impedance, not for the complex terminated impedance. Secondly, the measured results are transformed to the results of complex terminated impedance using the Advanced Design System. Fig. 6 shows the schematic for results transforming. The components in the yellow box are used to obtain a frequency-dependent complex load impedance. Fig. 6(b) shows the impedance curves of the load.

Figure 7 shows the measured frequency responses of fabricated WPD. For comparison, the simulated results are also added. It is observed that the dual-band characteristic can be clearly observed, and the measured results agree with the simulated ones. The first operating band is observed around 1 GHz,

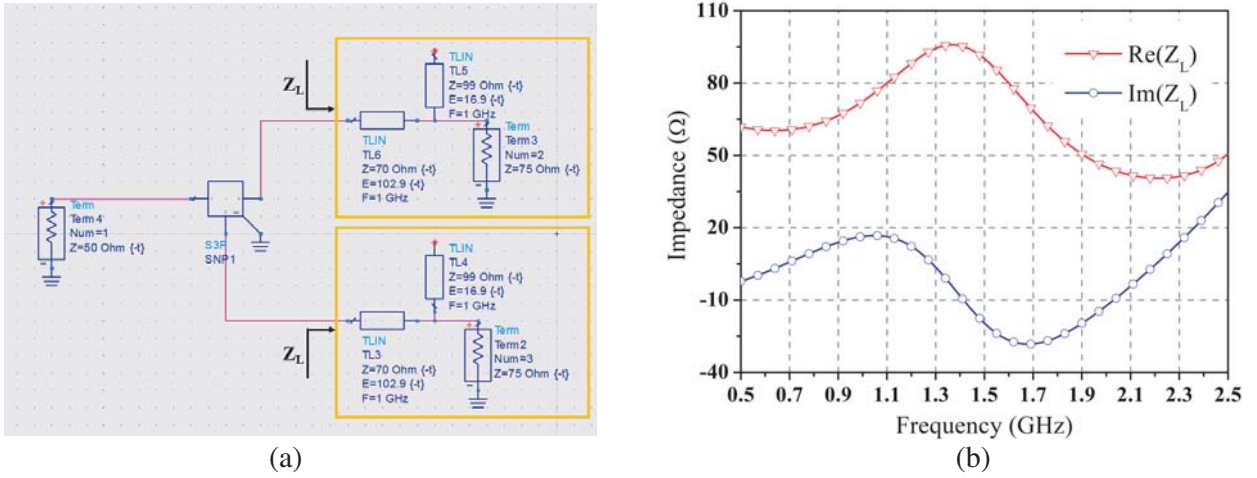


Figure 6. Data post-processing of the proposed WPD. (a) The schematic diagram. (b) The curves of load impedance.

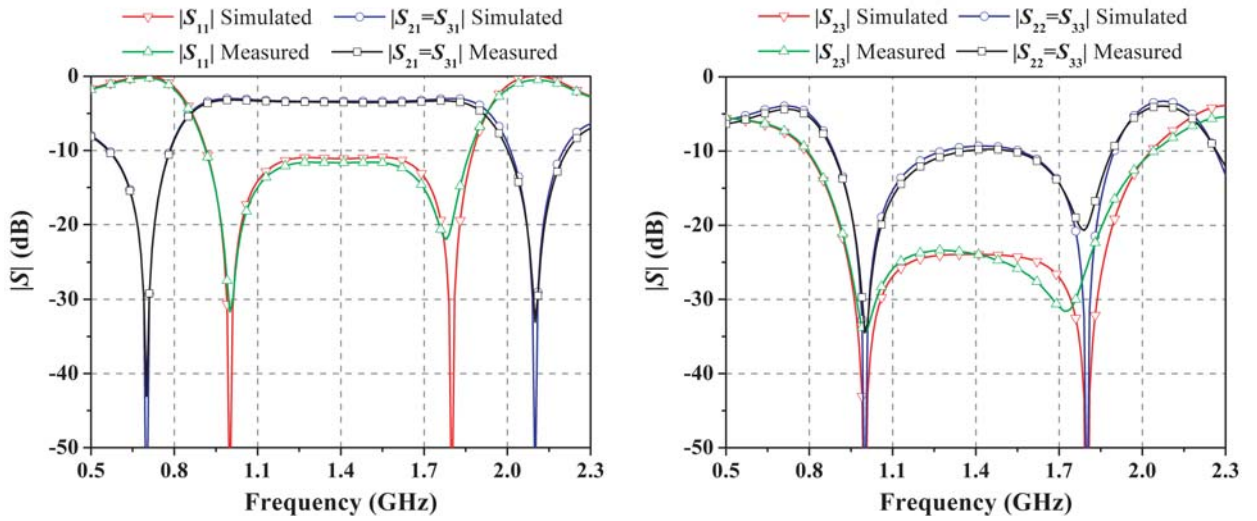


Figure 7. Measured and simulated frequency responses of the WPD.

with the input matching (S_{11}) – 31.7 dB, the output matching ($S_{22} = S_{33}$) – 34.5 dB, the isolation (S_{23}) – 34.5 dB, and the transmission ($S_{21} = S_{31}$) – 3.2 dB. The second operating band occurs around 1.8 GHz, with the input matching (S_{11}) – 19.9 dB, the output matching ($S_{22} = S_{33}$) – 20.3 dB, the isolation (S_{23}) – 25.6 dB, and the transmission ($S_{21} = S_{31}$) – 3.3 dB. Compared with the first band, the WPD has a degraded performance at the second band, which can be caused by the unequal phase constants associated with the coupled lines.

4. CONCLUSION

In the letter, a novel dual-band Wilkinson power divider terminated with a frequency-independent complex impedance is presented. Coupled lines are used to achieve perfect matching and isolation by providing different values of even- and odd-mode impedances. Analytical equations are derived, and design procedures are concluded as guidance. In order to verify the method, an experimental prototype is designed and fabricated. The measured results are in agreement with the simulated ones, which demonstrate that the proposed WPD can be a good candidate for microwave applications.

ACKNOWLEDGMENT

This work was supported in part by the National Natural Science Foundation of China under Grant 51809030 and Grant 61871417, in part by the China Postdoctoral Science Foundation under Grant 2017M611210, in part by the Doctor Startup Foundation of Liaoning Province under Grant 20170520150, and in part by the Fundamental Research Funds for the Central Universities under Grants 3132020207 and 3132020206.

REFERENCES

1. Park, M. and B. Lee, "A dual-band Wilkinson power divider," *IEEE Microwave and Wireless Components Letters*, Vol. 18, No. 2, 85–87, Feb. 2008.
2. Park, M., "Dual-band Wilkinson divider with coupled output port extensions," *IEEE Transactions on Microwave Theory and Techniques*, Vol. 57, No. 9, 2232–2237, Sept. 2009.
3. Wu, Y., Y. Liu, and Q. Xue, "An analytical approach for a novel coupled-line dual-band Wilkinson power divider," *IEEE Transactions on Microwave Theory and Techniques*, Vol. 59, No. 2, 286–294, Feb. 2011.
4. Wang, X., Z. Ma, and M. Ohira, "Theory and experiment of two-section two-resistor Wilkinson power divider with two arbitrary frequency bands," *IEEE Transactions on Microwave Theory and Techniques*, Vol. 66, No. 3, 1291–1300, Mar. 2018.
5. Ahn, H.-R. and S. Nam, "3-dB power dividers with equal complex termination impedances and design methods for controlling isolation circuits," *IEEE Transactions on Microwave Theory and Techniques*, Vol. 61, No. 11, 3872–3883, Nov. 2013.
6. Hallberg, W., M. Özen, D. Kuylenstierna, K. Buisman, and C. Fager, "A generalized 3-dB Wilkinson power divider/combiner with complex terminations," *IEEE Transactions on Microwave Theory and Techniques*, Vol. 66, No. 10, 4497–4506, Oct. 2018.
7. Monzon, C., "A small dual-frequency transformer in two sections," *IEEE Transactions on Microwave Theory and Techniques*, Vol. 51, No. 4, 1157–1161, Apr. 2003.